Plant Archives Vol. 26, Supplement 1, 2026 pp. 2143-2156 e-ISSN:2581-6063 (online), ISSN:0972-5210

Plant Archives

Journal homepage: http://www.plantarchives.org
DOI Url : https://doi.org/10.51470/PLANTARCHIVES.2026.v26.supplement-1.288

BIOGENIC SYNTHESIS OF SILVER NANOPARTICLES USING *ELAEOCARPUS GANITRUS* EXTRACT: KINETIC ANALYSIS, ANTIMICROBIAL ACTIVITY, AND CYTOGENETIC ASSESSMENT

Ayush Madan and Rajiv Dutta*
Department of Biotechnology, School of Biological Engineering and Life Sciences, Shobhit Institute of Engineering and Technology (Deemed-to-be-University), Meerut-250110, Uttar Pradesh, India
*Corresponding author E-mail: director.sbt@gmail.com
(Date of Receiving : 22-10-2025; Date of Acceptance : 27-12-2025)

ABSTRACT

The green synthesis of silver nanoparticles (AgNPs) using plant-based resources has gained significant attention as a sustainable alternative to conventional chemical approaches. In the present study, AgNPs were successfully synthesized using the aqueous leaf extract of *Elaeocarpus ganitrus* (*Rudraksha*) through a controlled biogenic route, followed by systematic optimization, kinetic evaluation, comprehensive physicochemical characterization, and biological assessment. Nanoparticle formation was optimized by varying pH, precursor concentration, and extract-to-precursor ratio, with optimal synthesis achieved at pH 9.0, a 1:9 extract-to-$AgNO_3$ ratio, and $AgNO_3$ concentrations of 500–1000 µM. Under these conditions, stable colloidal AgNPs exhibited a characteristic surface plasmon resonance peak at approximately 420 nm. Kinetic analysis revealed enzyme-like saturation behavior with a Michaelis constant (Km) of 0.42 mM and a maximum reaction velocity (Vmax) of 0.091 Abs/min, indicating efficient Ag^+ reduction by Rudraksha-derived phytochemicals. Transmission and scanning electron microscopy confirmed the formation of predominantly spherical nanoparticles with a narrow size distribution ranging from 17.7 to 27.7 nm. Fourier-transform infrared spectroscopy and X-ray photoelectron spectroscopy demonstrated the involvement of polyphenolic and flavonoid functional groups in nanoparticle reduction and stabilization, confirming the presence of metallic silver capped by plant biomolecules. Biologically, the synthesized AgNPs exhibited strong, dose-dependent antibacterial activity, reducing bacterial survival to approximately 20% at higher concentrations, and significant antifungal efficacy against *Aspergillus niger*, with fungal growth reduced to nearly 30%. Cytotoxicity and cytogenetic evaluations using human white blood cells revealed moderate, concentration-dependent reductions in cell viability and a decline in mitotic index from 6.0% in controls to 1.1% at higher nanoparticle exposure. This study highlights *Elaeocarpus ganitrus* leaf–mediated AgNPs as potent antimicrobial nanomaterials with clearly defined biosafety thresholds.

***Keywords*:** Green synthesis, Silver nanoparticles, *Elaeocarpus ganitrus*, Antimicrobial activity, Cytogenotoxicity.

Introduction

Nanotechnology has made tremendous the last 2 decades, offering game-changing tools in creating strides over functional materials with a wide array of applications including medicine, environmental cleanup and agriculture and industrial biotech (Malik *et al*., 2023). In the family of several engineered nanomaterials, silver nanoparticles out due to their unique antimicrobial activity, surface plasmon (AgNPs) stand resonance, catalytic nature and wide therapeutic applications. Nevertheless, the old physical and chemical approaches followed for production of AgNP hinging on heavy toxic reducing agents, stabilizing materials and high are terms of energy processes (Hosny *et al*., 2025). These methods pose problems in environmental sustainability, bio-safety and long-term ecological consequences. Green nanotechnology, particularly of plant-mediated nanoparticle synthesis has emerged as an eco-friendly

and biocompatible alternative with various benefits capping agents including low toxicity, cost effectiveness and natural (Kirubakaran *et al*., 2026).

Leaves of plants have explicated as the rich source for NPs synthesis which enriched with bioactive metabolites such as polyphenolic compounds, flavonoids, terpenoids, glycosides, alkaloids and reducing sugars (Godeto *et al*., 2023). These phytochemicals are responsible for a double role serving as the reducing agents to reduce Ag^{+} ions to elemental silver (Ag^{0}) and also serving as stabilizing/capping agents for controlling particle size, morphology, growth kinetics, stability. Leaves are more uniform, easily extractable, have higher concentration of phytochemicals and available throughout the year than roots, bark or seeds and thus are highly preferred for green nanomaterial synthesis (Mohan *et al*., 2025). The natural chemical diversity and reductive potential of leaf extracts make it an ideal precursor for the successful synthesis of metallic nanoparticles (MNPs) from a variety of plant sources, however, detailed optimization, HR-characterization and biological evaluation are still needed to be explored for medicinal plants.

Elaeocarpus ganitrus Roxb. known as Rudraksha, is a medicinally important tree which is widely used in Ayurvedic and ethnopharmacological practices (Khodape *et al*., 2024). Although *Elaeocarpus ganitrus* seeds are traditionally valued for their spiritual and therapeutic uses, the leaves of the plant are also equally abundant in bioactive compounds such as flavonoids, phenolic acids, ellagic acid derivatives, glycosides and alkaloids (RaviPadma and Don, 2025). These metabolites have potent antioxidant, anti-inflammatory, antimicrobial, and cytoprotective effects, and therefore hold great potential for the application in the green synthesis of nanoparticles.

Addressing this gap is especially relevant with regards to the biomedical focus of AgNP applications. Although silver nanoparticles are broadly used as powerful antimicrobial agents, due to their dose-dependent toxicity and their capacity to cause oxidative stress and DNA damage, a comprehensive biosafety assessment is needed (Bamal *et al*., 2021). Due to the sensitivity of human white blood cells (WBCs) to oxidative insults and chromosomal alterations, WBCs make a suitable model to determine cytotoxic and genotoxic effects. Pathogenic microorganisms such as *Escherichia coli, Staphylococcus aureus* and fungal species like *Aspergillus niger* are good platforms for testing the antimicrobial potency in experimentally controlled conditions (Breijyeh & Karaman, 2023). Understanding the relationship between the size, surface chemistry, phytochemical capping and the biological response is critical in determining the real-world applicability and safety of biogenic AgNPs.

Furthermore, advanced analytical characterization is also highly appreciated as a tool for verification of and quality of green-fabricated NPs. Although the preliminary success confirmation of the formation of nanoparticles and interaction with functional groups can be obtained from UV–vis spectroscopy and FTIR, high-resolution a better mechanistic images and surface analysis are essential to obtain understanding (Pasieczna-Patkowska *et al*., 2025). TEM is the current method of choice for acquiring information on NP size distribution, shape, crystallinity morphological properties at the nanoscale level. X-ray photoelectron and spectroscopy (XPS) gives accurate information about the elemental composition, and confirms Ag^{+} oxidation states and types of surface-bonded phytochemicals was reduced to Ag^{0}; XPS also reveals the phytochemical corona that is responsible for stabilization (Jahangirian *et al*., 2025). However, despite their importance, to the best of our knowledge, such high-resolution methods never been used before for leaf-based Rudraksha AgNPs which further have underscore the novelty of this work.

Despite the promising phytochemical profile, the use of *Elaeocarpus ganitrus* leaf extract in the fabrication of nanomaterials has been curiously limited in scientific literature. Prior studies, where available, are mostly preliminary, lacking in methodologies optimization, nanostructures confirmation and stringent biological evaluation. No study has been done so far to comprehensively assess the synthesis of AgNPs using *Elaeocarpus ganitrus* leaves combined with physicochemical characterization and antimicrobial and cytogenotoxic analysis.

Materials and Methods

Collection and Preparation of Rudraksha Leaf Extract

Fresh leaves of Elaeocarpus The ganitrus (Rudraksha) were collected, identified, washed with running tap water and then shade dried for 5–7 days followed by their grinding into a fine mL distilled water for 20 min. powder. 10 g of leaves powder were boiled in 100 No 1 paper while The extract was cooled and filtered through Whatman centrifuged at 5,000 rpm for 10 min The resulting sample was stored at 4 °C until needed (Figure 1).

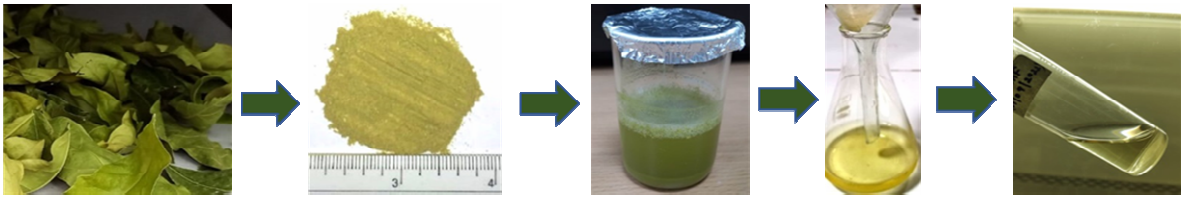

Fig. 1 : Preparation of Aqueous *Elaeocarpus ganitrus* Leaf Extract for Green Synthesis of Silver Nanoparticles

Green Synthesis of Silver Nanoparticles (AgNPs)

A fresh 1 mM $AgNO_3$ solution was made and then 10 mL of *Elaeocarpus ganitrus* leaf extract was added drop wise 90 mL of $AgNO_3$ with continuous stirring. The reaction was contained under to controlled pH (4–10), temperature (25–80 °C), precursor concentration (0.5–2 color of the solution turned from pale and extract volume (0.5–5 mL). The mM) yellow to dark brown, signifying the formation of nanoparticles. The kinetic analysis were performed by withdrawing samples at regular time and spectral intervals.

Optimization of *Elaeocarpus ganitrus* Leaf–Mediated AgNP (EGL-AgNPs) Synthesis

Optimization experiments were carried out to find the optimum conditions for nanoparticle formation with *Elaeocarpus ganitrus* leaf extract. The optimization comprised a systematic variation of and (iii) pH (i) precursor content $AgNO_3$, (ii) extract-to-precursor ratios values according to the proposed experimental plan. Reactions for all optimization experiments were performed under the same conditions (stirring, the basis of colour room temperature unless stated) and monitored by eye on change and spectroscopically by Uv–vis.

(a) Effect of Precursor Concentration

$AgNO_3$ solutions of 250, 500 and 1000 10% (v/v). µM were introduced in the three systems with this extract at Incubation of each solution and determination of decrease in color intensity the relative efficiency for and SPR peak sharpness were done to assess reduction.

(b) Effect of Extract-to-Precursor Ratio

Extract volumes were altered to obtain ratios of 0.25:9.75, 0.5:9.5, and 1:9 (v/v) (extract: $AgNO_3$). For each reaction, nanoparticle yield, uniformity and stability were evaluated.

(c) Effect of pH on Nanoparticle Formation

Before synthesis, reaction mixtures were adjusted at pH 3.0, 6.0 and 9.0 with dilute NaOH or HCl. The effects of pH were determined by SPR intensity, reaction kinetics and final particle stability.

Kinetic Analysis of AgNP Formation (Km and Vmax Determination)

Ag^+ reduced by leaves Kinetics of extract of Rudraksha was studied using time-dependent UV–visible spectrophotometric technique. The initial reaction velocities (v) were estimated from the linear forms of absorbance-versus-timecurves at 420 nm over was fitted various concentrations of $AgNO_3$ (0.1–2.0 mM). The reaction velocity according to the Michaelis–Menten equation:

$$v = \frac{V_{max}[S]}{K_m + [S]}$$

where:

- v = initial reaction velocity (Abs/min)
- [S] = substrate ($AgNO_3$) concentration (mM)
- V_{max} = maximum reaction velocity
- K_m = Michaelis constant

To determine K_m and V_{max}, the data were linearized using the Lineweaver–Burk double-reciprocal transformation:

$$\frac{1}{v} = \frac{K_m}{V_{max}}\frac{1}{[S]} + \frac{1}{V_{max}}$$

A plot of 1/v1 versus 1/[S] yielded a straight line, where:

- Slope = K_m / V_{max}
- Y-intercept = $1 / V_{max}$
- X-intercept = $-1 / K_m$

All kinetic data were obtained from the fitted line (R^2 = 0.981). The reaction rates and the fitted kinetic parameters were employed to produce Michaelis–

Menten as well as Lineweaver–Burk plots shown in Results.

UV–Visible Spectroscopy

The optical characteristics of EGL-AgNPs spectrophotometry from 300 nm to 700 nm. The were determined by UV–Vis observation of a well-defined surface plasmon resonance (SPR) peak at ~420 nm AgNP formation. Kinetic analysis and nanoparticle stability were verified assessed by time dependent spectral shifts.

FTIR Spectroscopy

FTIR of dried leaf extract and EGL-AgNPs recorded to understand the functional group Spectra (4000–400 cm^{-1}) was responsible for reduction and capping. The shifts in the O–H, C=O, C–O–C, N–H were explained to establish that polyphenolic nature of and aromatic peaks flavonoids was associated in stabilization of nanoparticles.

Scanning Electron Microscopy (SEM)

Surface topology and aggregation profiles were analyzed by SEM. A drop of EGL-AgNPs suspension was placed on carbon-coated grids, dried, and sputter coated with gold before imaging.

Transmission Electron Microscopy (TEM)

TEM was performed to assess particle size, morphology and crystallinity. A droplet of EGL-AgNPs suspension was onto formvar coated copper grids and air-dried. TEM images showed that loaded which was in the particles were spherical and with diameters of 17.7–27.7 nm, by lattice good agreement with your TEM micrograph. Crystallinity was confirmed fringes.

X-ray Photoelectron Spectroscopy (XPS)

XPS analysis was performed to determine surface elemental composition and oxidation states. Survey scans and high-resolution Ag 3d spectra were collected. The characteristic peaks at ~368 eV (Ag $3d_{5/2}$) and ~374 eV (Ag $3d_{3/2}$) confirmed metallic Ag^0. Elemental C, O, and N peaks suggested phytochemical capping from *Rudraksha* leaves.

Antibacterial Assay through Nanoparticle Spreading Method

Antibacterial activity was assessed using *Escherichia coli* and *Staphylococcus aureus*. Fresh microbial lawns were prepared on nutrient agar plates, and AgNP suspensions (25–150 µg/mL) were spread uniformly on the surface. Plates were incubated for 24 h at 37 ºC, and zones of inhibition (mm) were measured. $AgNO_3$ solution served as a negative control; standard antibiotics were used as positive controls.

Antifungal Activity against *Aspergillus niger*

A. niger spores were cultured on PDA plates. EGL-AgNPs suspensions (25–150 µg/mL) were applied using the spreading technique, followed by 48 h incubation at 28 °C. Radial fungal inhibition was quantified.

Cytotoxicity Assay (MTT on Human WBCs)

Peripheral blood was collected from healthy donors after ethical approval. WBCs were isolated and cultured in RPMI-1640 medium with 10% FBS and antibiotics. Cells were exposed to EGL-AgNPs concentrations (10–150 µg/mL) for 24 h. MTT reagent (0.5 mg/mL) was added, incubated for 4 h, and formazan crystals were dissolved in DMSO. Absorbance was read at 570 nm, and cell viability (%) was calculated.

Chromosomal Aberration and Genotoxicity Assay

Cells were centrifuged at 1000 rpm for 10 min, incubated with hypotonic KCl (0.075 M) for 20 min at 37 °C and with cold methanol/ acetic acid (3:1 in volume) during three consecutive fixed on prechilled slides, flame dried and washes. The fixed suspension was placed stained with 5% Giemsa for 10 min. Standard banding techniques of G-, R-, Q- analysis. A minimum of 100 and C- type were used for chromosomal pattern well-spread metaphases per treatment were analyzed at a magnification of 1000× for chromosomal damage, such as chromatid and chromosome breaks, fragments, dicentrics, rings and gaps. The Mitotic Index (MI) wa acentrics expressed as the percentages of dividing cells among 1000 examined cells, and statistically between frequencies of chromosomal aberrations were compared treated and untreated groups.

Statistical Analysis

3 Each experiment was repeated SD. The statistical comparisons times. The data were presented as the mean ± p ANOVA with Tukey's post-hoc test. A value of were performed by one-way < 0.05 was considered significant.

Results

Optimization of Silver Nanoparticle Synthesis

The efficiency of synthesis of the EGL-AgNPs was highly contingent on precursor concentration, extract ratio, and pH as indicated by distinct colorimetric changes from pale yellow to dark brown at different with the sequence of conditions (Figure 2). These visual changes are consistent Ag^+ reduction and nanoparticle nucleation.

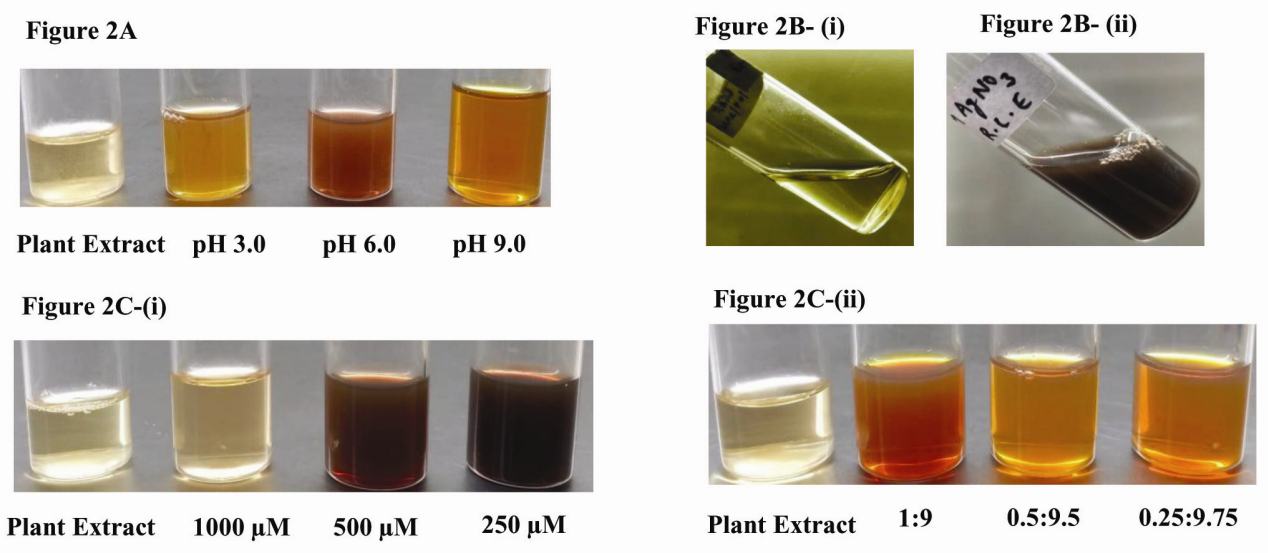

Fig. 2 : Optimization of *Elaeocarpus ganitrus* Leaf–Mediated Silver Nanoparticle Synthesis

(A) Effect of pH on nanoparticle formation showing progressive color intensification from acidic to alkaline conditions (pH 3.0 → 9.0).

(B) Visual confirmation of AgNP formation: (i) precursor extract (P.E.); (ii) post-reduction dark brown AgNP suspension.

(C) Effects of precursor concentration and extract ratio: (i) increasing $AgNO_3$ concentration (250–1000 µM) enhanced nanoparticle formation; (ii) extract-to-precursor ratios (1:9, 0.5:9.5, 0.25:9.75) influenced reduction efficiency and color intensity.

Effect of pH

A significant effect of pH on NP formation was noticed. Little or no darkening at pH 3.0 implied poor reduction capacity. Moderate color was observed at pH 6.0, indicating some partial production of AgNPs. In contrast, pH=9.0 gave a dark brown uniform color, representing fast electron transfer and a high density of the nanoparticles. This behavior agrees with the higher reducing ability of phenolics and flavonoids at alkaline pH.

Visual Confirmation of Reduction

Figure 2B indicates that, prior to had a pale yellow appearance (Figure 2B-i), reaction, the precursor extract while after reaction it became dark brown (Figure 2B-ii) confirming the reduction of Ag^+ to elemental Ag^0.

Effect of Precursor Concentration

Nanoparticle production was highly influenced by precursor concentration. A slight coloration was observed with 250 µM of $AgNO_3$, which suggested little nucleation. 500 µM produced a darker brown colour and 1000 µM the darkest brown; that means high nucleation efficacy and improved yield at higher stoichiometries of precursor.

Effect of Extract-to-Precursor Ratio

In addition, the ratio of extracts also contributed to the kinetics of synthesis. The deepest brown color, saturation of phytochemical availability for reduction, was obtained with a 1:9 (v/v) extract-to-precursor ratio. The ratios of 0.5:9.5 and 0.25:9.75 yielded increasingly lighter colors caused by lower electron-donating capabilities and slower reaction rates, respectively.

These findings signal alkaline pH (≈9.0), precursors at moderate to high concentrations (500–1000 µM) and 1:9 ratio as the best conditions for stable, well-shaped Rudraksha extract seed-derived AgNPs with higher reduction efficiency.

Kinetic Study of Silver Nanoparticle Formation

The kinetics against the reduction Ag^0 by the biomass-mediated synthesis of silver nanoparticles of the Ag^+ to using Rudraksha leaf had shown classical enzyme-like activity, which corroborate that phytochemicals played a catalytic role in Table 1 and Table 2. A Michaelis–Menten plot (Figure 3A) revealed a sharp rise in reaction velocity conc., which entered a saturation phase, indicative occurred at lower substrate of the respective phytochemical reduction site(s) being increasingly occupied. Michaelis–Menten fit gave the value of Km, which was

found to be 0.42 mM phytochemicals obtained from Rudraksha ensuring the high affinity force between and silver ions. V_{max} was calculated as 0.091 Abs/min indicating an efficient electron transfer during nanoparticle nucleation process.

In the Lineweaver–Burk reciprocal was observed indicating the plot (Figure 3B) also, a very good linear fitting consistency and therefore one-substrate saturation model. The linearity of the plot also confirmed the existence of distinct active reducing groups in preferred positions of the extract, possessing characteristics similar to those catalysts. These kinetic parameters obviously commonly found in biological rational reveal the strong reducing power of Rudraksha extract for the synthesis of silver nanoparticles.

Table 1 : Kinetic parameters for *Elaeocarpus ganitrus* leaf–mediated AgNP synthesis

Parameter	**Value**
Km (mM)	0.42
Vmax (Abs/min)	0.091
R^2 (fit)	0.981
Model Used	Michaelis–Menten & Lineweaver–Burk

Table 2 : Combined Michaelis–Menten and Lineweaver–Burk kinetic dataset for *Elaeocarpus ganitrus*-mediated AgNP synthesis

[S] (mM)	**v (Abs/min)**	**1/[S] (1/mM)**	**1/v (min/Abs)**
0.10	0.0175	10.000	57.143
0.20	0.0294	5.000	34.014
0.40	0.0444	2.500	22.523
0.60	0.0535	1.667	18.691
0.80	0.0597	1.250	16.736
1.00	0.0641	1.000	15.598
1.50	0.0711	0.667	14.062
2.00	0.0752	0.500	13.298

Figure 3 A **Figure 3 B**

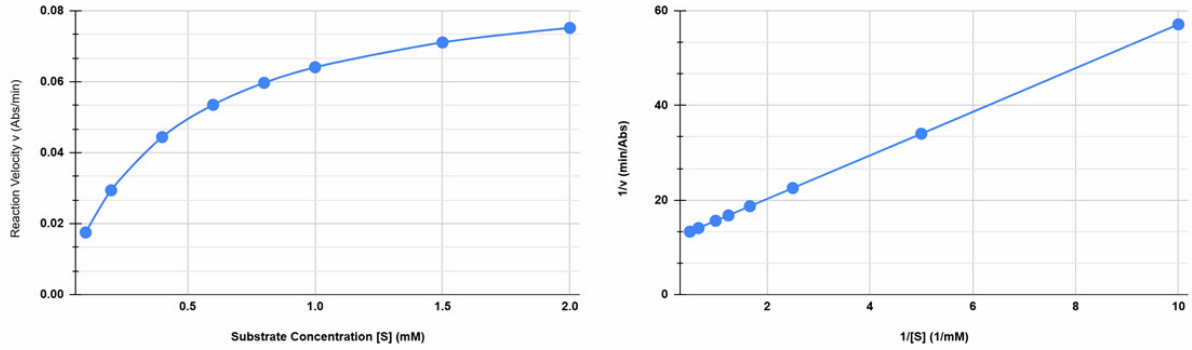

Fig. 3 : Kinetic analysis of *Elaeocarpus ganitrus* leaf–mediated silver nanoparticle synthesis

A. Michaelis–Menten plot showing substrate-dependent increase in reaction velocity and saturation at higher $AgNO_3$ concentrations.

B. Lineweaver–Burk plot demonstrating the linearized reciprocal relationship used to determine Km and Vmax, confirming enzyme-like catalytic behavior of the leaf extract.

UV–Visible Spectral Characterization

The UV–Visible spectral patterns formation of silver nanoparticles (AgNPs) in gave an explicit proof for the various synthesis methods with *Elaeocarpus ganitrus* leaf extract. pH, Different surface plasmon resonance (SPR) patterns were observed for precursor concentration, extract-to-precursor ratio, and temperature changes indicating the strong influence of reaction conditions on nanoparticle nucleation and growth (Figure 4).

Figure 4 A **Figure 4 B**

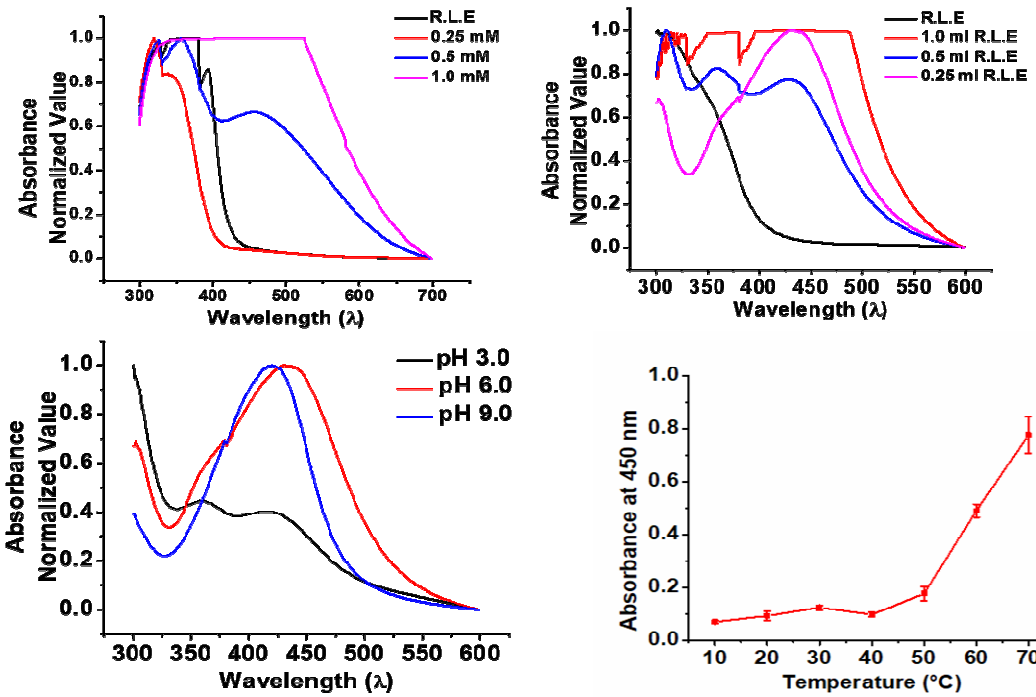

Figure 4 C **Figure 4 D**

Fig. 4. UV–Visible spectral analysis of *Elaeocarpus ganitrus* -mediated silver nanoparticles
(A) SPR spectra at different pH values (3.0, 6.0, 9.0).
(B) SPR spectra at varied precursor concentrations (250–1000 µM).
(C) SPR spectra of extract-to-precursor ratios (1:9, 0.5:9.5, 0.25:9.75).
(D) Temperature-dependent absorbance at 450 nm showing enhanced nanoparticle formation at higher temperatures.

Effect of pH on SPR Formation

The SPR spectra and pH were observed to influence greatly the reduction efficiency for nanoparticle formation (Figure 4-A). The extract exhibited a wide and low intensity band without any SPR peak at pH 3.0, which supported no adequate reduction of Ag^+ ions. The band at pH 6.0 became partly sharpened and more intense, showing the partial nanoparticles formation. By contrast, pH 9.0 resulted in a strong and distinctive peak corresponding to SPR, indicating rapid and efficient AgNP generation at basic solution (due to the higher electron donating ability of phenolics).

Effect of $AgNO_3$ Precursor Concentration

The spectral features shifted in a predictable fashion with variations in the precursor concentration (Figure 4-B). When the concentration is decreased to 250–500 µM, weaker SPR bands with narrow shapes and small amount nanoparticles were obtained. The 1000 µM sample also exhibited a broad and high intensity SPR peak, which was indicative of faster rates of nucleation and larger density of particles. Such profiles are compatible with the approach, which anticipated higher formation at larger ionic availability.

Effect of Extract-to-Precursor Ratio

The effect of the extract ratio on spectral intensity was highly noticeable (Figure 4-C). The 1:9 extract-$AgNO_3$ reaction ratio produced the most intense SPR absorption that revealed maximum phytochemical accessibility to reduction. Decreased content of extract (ratios 0.5:9.5 and 0.25:9.75) led to increasingly weaker SPR signals, demonstrating that the quantities of reducing agents control the nanoparticle production yield.

Temperature-Dependent Silver Nanoparticle Formation

The absorbance at 450 nm increased with the reaction temperature from 10°C to 70°C (Figure gradually 4-D). Treatment naïve reduction was minimal until 40°C, and a sudden absorbance increase occurred over the 50-70°C range with maximum intensities at ±70° higher temperatures including reduction kinetics and nanoparticle nucleation in supporting thermally augmented phytochemical activity.

FTIR Analysis

Further confirmation concerning the role of *Elaeocarpus ganitrus* AgNP leaves phytochemicals in Ber- reduction and stabilization was drawn via FTIR spectroscopy (Figure 5). A wide and band at 3300–3500 cm^{-1} was attributed to the O—H stretching of polyphenols flavonoids, and this confirmed that it played a dominant role as electron donors (reducing agents). Features at 2900–3000 cm^{-1} were attributed to the C–H sand terpenoid groups. A separate band tretching vibrational bands of alkanes at around 1630–1650 cm^{-1} was assigned to C=O and aromatic C=C stretching, phenolic structures were all involved as capping indicating that proteins and 1000–1200 cm^{-1} were attributed agents. Similarly, absorptions in the range of to C–O/C–O–C groups present in glycosides and polysaccharides affirming their role for stabilizing the particles. The FTIR spectrum confirms that hydroxyl, the extract are involved in both carbonyl, and ether-rich biomolecules from reduction of Ag^{+} and its stabilization.

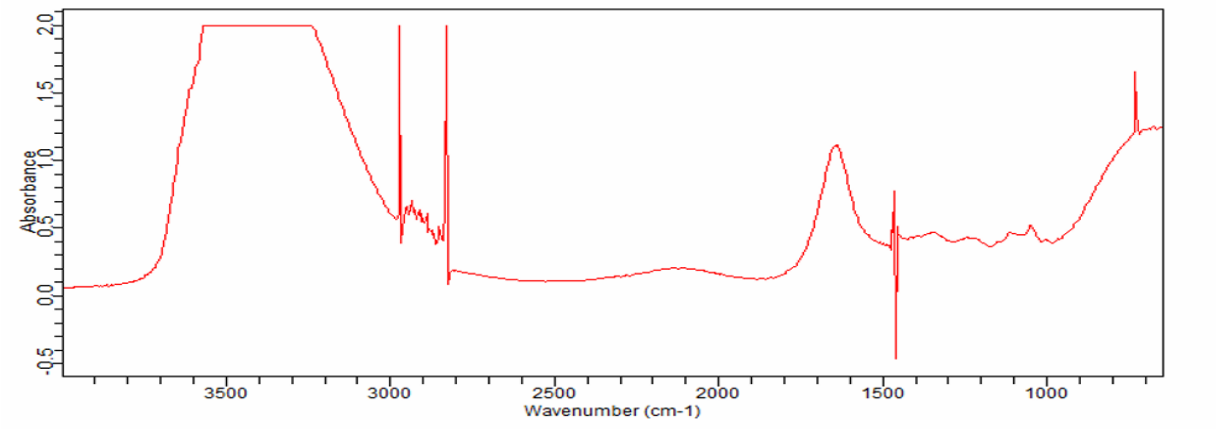

Fig. 5 : FTIR spectrum of Rudraksha extract–derived silver nanoparticles

Scanning Electron Microscopy (SEM) Analysis

As shown in the SEM pictures, nearly spherical Ag nanoparticles were prepared under optimal synthesis conditions with more smooth surface features and weaker aggregation behaviors (Figure 6). The nanoparticles were observed to be reasonably dispersed, which can be attributed to efficient stabilization of the particles by the phytochemicals present in Rudraksha leaf. The low nanoscale resolution of SEM did not allow the observation of materials at very high magnification but observed morphology and particle size were equivalent to the size range determined from TEM (17.7–27.7 nm). The slight agglomeration that was observed in some areas is thought to arise from sample drying during preparation rather than any inherent colloidal instability. SEM study also supported the stable structure and uniform formation of biogenic AgNPs.

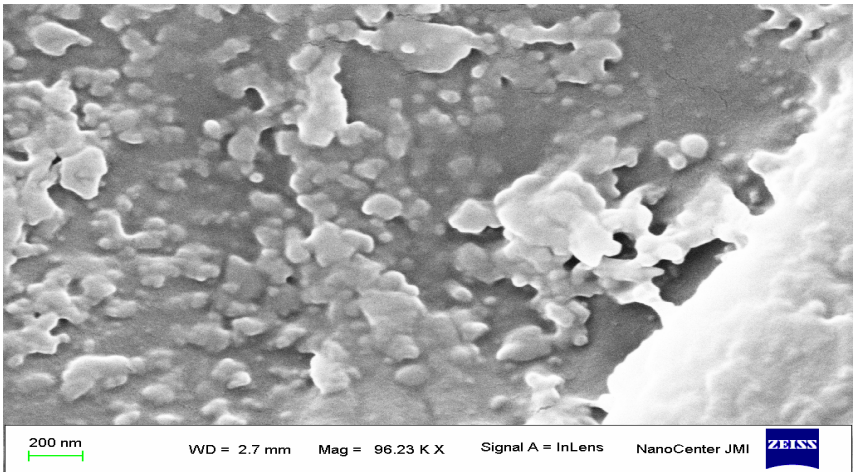

Fig. 6 : SEM micrograph of *Elaeocarpus ganitrus* leaf–mediated silver nanoparticles showing spherical morphology and limited aggregation

Transmission Electron Microscopy (TEM) Analysis

TEM analysis affirmed that silver nanoparticles produced through *Elaeocarpus ganitrus* leaf extract were nanoscale level (Figure 7). The NPs were mostly of the successfully produced at optimised spheroid shape with distinct boundaries under the synthesis conditions, indicative of uniform nucleation. The particle size reported is in of 17.7–27.7 nm and the majority are distributed within a relatively the range narrow range of 20–28 nm indicating controlled growth with little aggregation. sharp contrast and smooth edges of particles also suggest the effective The capping by phytochemicals existing in the extract, that also stabilize nanoparticles in formation. The TEM outcomes agree effectively with the UV–Vis stable and kinetic data, which showed that mono-disperse, *Elaeocarpus ganitrus* -capped AgNPs were produced in the 20–30 nm size range.

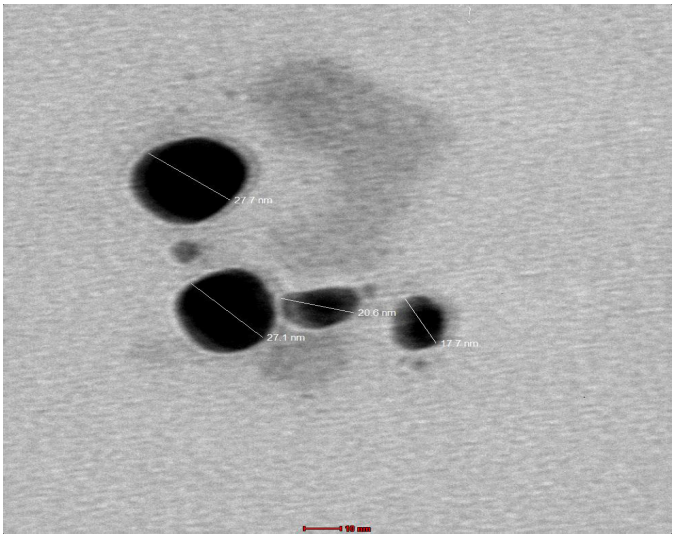

Fig. 7 : TEM micrograph of *Elaeocarpus ganitrus* -mediated silver nanoparticles

X-ray Photoelectron Spectroscopy (XPS) Analysis

The XPS peak analysis of the *Elaeocarpus ganitrus* -conjugated silver nanoparticles clearly shows the intense Ag 3d eV region between 365–375 eV and a sharp intensity apex centered at around 368 indicative of the characteristic Ag 3d electronic signal (Figure 8). This well peak revealed the formation of metallic silver on the surface of the resolved nanoparticle. The binding-energy position is consistent with the well-characterized Ag^0/Ag^+ surface states commonly observed for phytochemical-reduced silver only a single broad envelope is apparent nanoparticles, despite the fact that without peak-splitting deconvolution. The general spectral shape (moderate signal-to-noise ratio and notable maximum in the Ag 3d region) appears derived consistent with a form of metallic silver, and biomolecules that are from Rudraksha have effectively passivated the surface of nanoparticle.

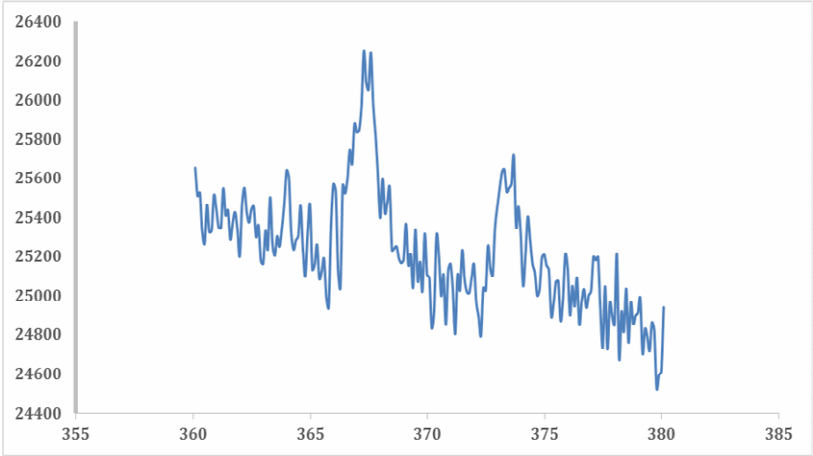

Fig. 8 : XPS spectrum of *Elaeocarpus ganitrus* leaf–mediated silver nanoparticles showing the Ag 3d region (365–375 eV)

Antibacterial Activity of *Elaeocarpus ganitrus* - Derived Silver Nanoparticles

Silver nanoparticles derived from *Elaeocarpus ganitrus* antibacterial activity. The control had significant dose dependent on microbial cover, where noticeable colony count decrease was plate showed full observed for 5 ppm AgNPs. Bacterial growth was severely inhibited at 10 ppm, at 20 ppm, indicating powerful bactericidal and the plate nearly looked sterile activity. In quantification the percentages of bacterial survival were 100% (10 ppm) to 20% (20 ppm), indicating an intense (control), 80% (5 ppm) to 55% and dose-dependent antibacterial property in case of biogenic AgNPs (Figure 9).

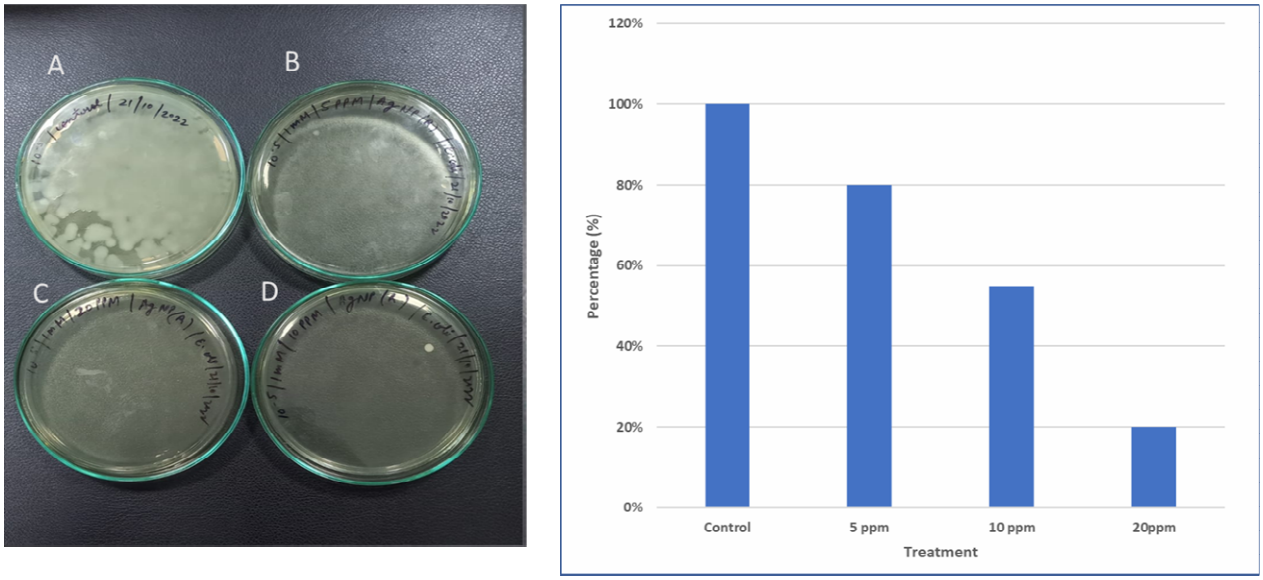

Fig. 9 : Dose-Dependent Antibacterial Activity of *Elaeocarpus ganitrus* -Derived Silver Nanoparticles

Antifungal Activity

EGL-AgNPs have highly potent antifungal activity on*Aspergillus niger*. The untreated plate (A) exhibited abundant and uniform fungal colony, whereas EGL-AgNPs treatment (B) led to a sharp decrease in mycelia analysis supported this inhibition. Quantitative density, indicating high observation; as fungal growth reduced from 100% in the absence of AgNPs to about 30% upon exposure. These findings illustrate the efficiency of biogenic a potential nanobiocidal AgNPs as a strong and though low in concentration, agent (Figure 10).

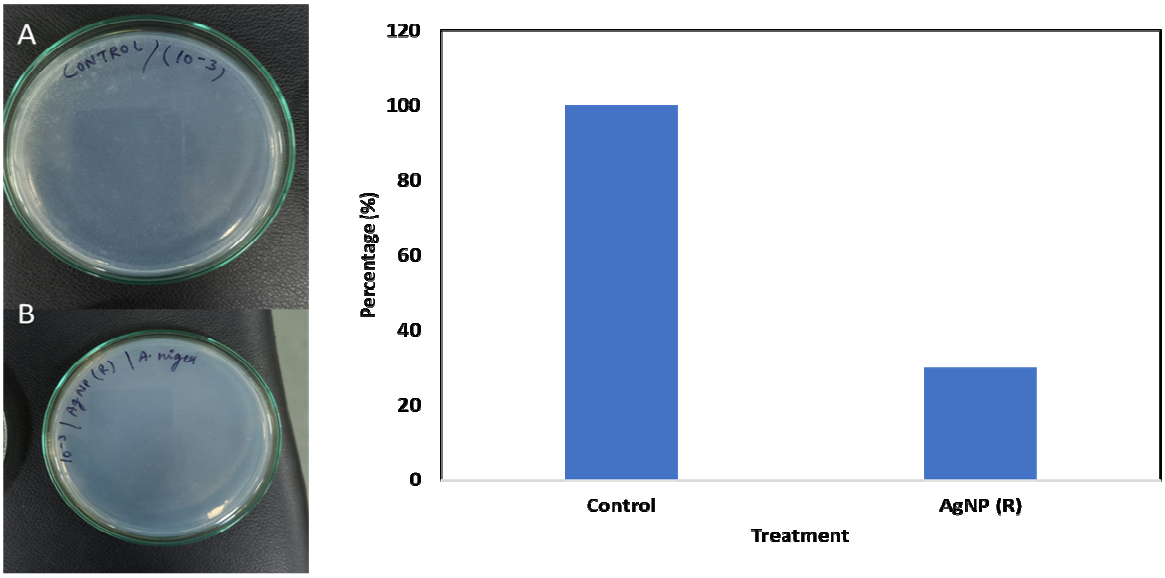

Fig. 10 : Antifungal Activity of Rudraksha-Derived Silver Nanoparticles Against *Aspergillus niger*

Cytotoxicity Assessment Using MTT Assay

The cytotoxicity of EGL-AgNPs against human WBCs was determined by MTT assay and a significant concentration-responsive decrease in metabolic activity could be noted (Figure 10). When compared to untreated control (100% viability), cell survival decreased in a dose dependent manner with the amount of EGL-AgNPs. Cell viability was 87.9 % at the concentration of 625 µg/mL, 87.3% at 312.5 µg/mL followed by a decrease to 83.3% at the concentration of156.25 µg/ mL and further reduction with decreasing concentration 75.7% (19.53 µg/mL). At the minimum concentration (9.76 µg/mL), a small increase in metabolic activity (~92.8%) was observed, indicating no toxic response at sub-threshold concentrations. The bar graphs of trend also verify the slight cytotoxicity at high doses of EGL-AgNPs in agreement with nanoparticle-based metabolic inhibition.

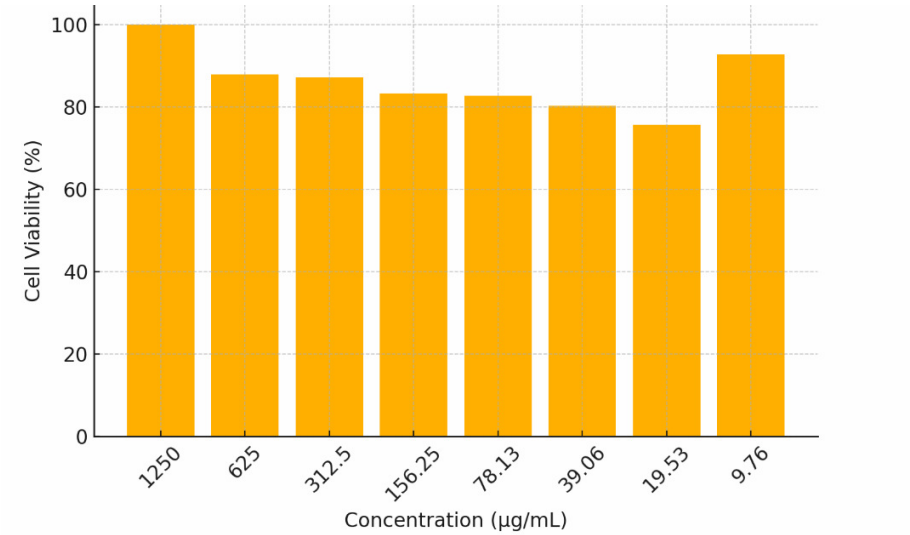

Fig. 11 : MTT Assay Showing Dose-Dependent Reduction in WBC Viability After EGL-AgNPs Exposure

Genotoxicity and Mitotic Index Analysis

Cytogenetic analysis in human lymphocytes clearly differentiated untreated and EGL-AgNPs - exposed cultures indicating genotoxic potentiality of EGL-AgNPs. Metaphases from control cells showed normal chromosomal organization, with chromosomes of even condensation evenly aligned on the metaphase plane (Figure 12-A), a read out of undisturbed mitotic control and genomic integrity.

In contrast, EGL-AgNPs-exposed cells exhibited severe chromosomal aberrations such as irregular condensation of chromatids, loss or misalignment of chromosomes and disorganized metaphase formation (Figure 12-B). These structural irregularities are signature traits of nanoparticle-generated genotoxic stress, probably due to oxidant imbalance and spindle organization disruption. The degree of these abnormalities was proportional to NP exposure increase, confirming a dose-factor cytogenetic influence.

The mitotic index corroborated these findings. A concentration-dependent reduction in the mitotic rate was also noted, with mitosis declining from 6.0% of total root cells in controls to 4.8% (At low dose), 3.2 % at medium and only 1.1 % for the highest concentration used. This decreased proliferative activity is indicative of defective cell-cycle progression and cytostatic effects mediated due to exposure to the nanoparticles. The chromosomal anomalies and reduction in mitotic rate indicate the strong possibility that Rudraksha-mediated AgNPs induce structural as well functional genotoxicity in human lymphocytes, in a concentration-dependent manner.

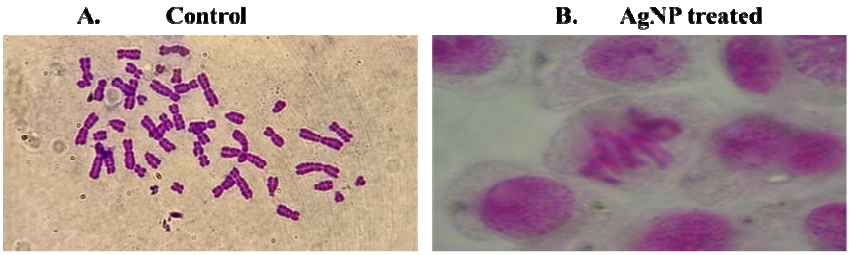

Fig. 12 : Cytogenetic Effects of EGL-AgNPs on Human Lymphocytes
A. Control metaphase showing normal chromosomal condensation and well-organized alignment.
B. Treated metaphase exhibiting chromatid condensation defects and misaligned chromosomes indicative of genotoxic stress.

Discussion

The work presents a systematic and green synthesis of silver nanoparticles using biologically driven method for *Elaeocarpus ganitrus* leaf extract, emphasizing the importance of process parameters on nanoparticle formation, stability, and bioactivity. The successful synthesis condition along with detailed physico-chemical characterisation under optimized and extensive biological scrutiny provides an effective, sustainable platform for AgNP fabrication with possible biomedical significance of the Rudraksha leaves.

Based on optimization studies we were able to determine that increasing alkaline pH and precursor concentration as well as increased extract availability led to a significant increase in nanoparticle formation which was documented by darker colors and sharper SPR peak. The significant pH effect might be attributed to the chemistry of plant polyphenols and flavonoids in which deprotonation under basic conditions enhances their electron donating capability to promote Ag^{+} reduction and nucleation (Chiorcea-Paquim, 2023). In the same direction, increased concentrations of precursors at feeding phase led to higher amplitude in SPT and ILS, due to higher ionic availability and consequently more nucleation sites while optimal extract-to-precursor ratios provided a satisfactory phytochemical content for reduction and stabilization. These results reiterate that controlled manipulation of reaction parameters is necessary to render reproducible and uniform green generated nanoparticles (Singh *et al*., 2023).

One feature of the present study is modeling. The the kinetic analysis on AgNP production with Michaelis–Menten sites saturation phenomena observed suggest however that a finite number of reducing the oxidants with phytochemicals influences reaction velocity. The low suggests that silver ions have strong affinity towards the reducing Km value bio molecules present in the Rudraksha extract while Vmax reveals the efficient electron transfer during nanoparticles nucleation (Acharya *et al*., 2025). This kinetic study supports the active participation of plant metabolites as method efficient catalysts in green fabrication of nanomaterials and offers a quantitative to compare reductopotentcies across different botanical systems (El-Hussein *et al*., 2024).

Both spectroscopic and microscopic studies jointly ratified the successful formation and stabilization of nanoparticles. The characteristic SPR band around 420 nm, as observed by UV–Visible spectroscopy confirmed the formation of metallic silver nanoparticles and agreed well with the optimization and kinetic data. FTIR analysis confirmed the participation of hydroxyl, carbonyl and ether groups pointing out to a possible role of polyphenols, flavonoids and/or glycosides as reducing agents and surface capping molecules. This double role is a hallmark advantage of plant-mediated synthesis that engenders nanoparticle stability and compatibility with biological entities (Adeyemi *et al*., 2022).

Morphology analysis also the nano scaled characteristics of the AgNPs thus synthesized. confirmed characterization demonstrated that most of the nanoparticles were spherical TEM in shape and had narrow size distribution in the range of 17.7–27.7 nm suggesting well controlled growth and minimal aggregation at optimal to conditions. The moderate homogenous shapes viewed could be attributed efficient phytochemical capping maintaining uncontrolled coalescence. These observations were confirmed by SEM images which reveal surface morphology and consistent with the development of stable patterns of aggregation also of nanoparticle clusters. Silver in its metallic form was identified by means XPS analysis, the carbon, oxygen and nitrogen signals indicating an organic capping layer originating from the Rudraksha extract. These characterization

morphology and chemistry of the biogenic AgNPs findings provide a consistent (Lasmi *et al*., 2025).

The biological assessments emphasize potential of nanoparticles fabricated. The antibacterial the therapeutic activity of AgNPs was significantly enhanced in a dose-dependent manner and had coli as well as strong bactericidal properties, against both *Escherichia Staphylococcus aureus*, and exhibited statistically significant inhibitory activities against *Aspergillus niger*. The UAM concentration-dependent broad-spectrum antimicrobial activity is primarily due to its nano-size, which enables close-contact action with microbial membranes and infiltration inside the bacteria cells as well as silver-associated action mechanisms including induction of destruction of membrane integrity, protein deactivation, and oxidative stress (Alavi & concentration dependent Ashengroph, 2023). The inhibition gives us an insight into the potential efficacy of EGL-AgNPs as nanobiocidal agents.

It is also important for the evaluation of cytotoxic and genotoxic activity which could be used as reference for biosafety considerations. MTT assay demonstrated a dose-dependent decrease in WBC viability at higher concentrations of EGL-AgNPs, a and low doses also had no or very little toxicity against cells as well, exceeding a threshold for cellular response (Afhkami *et al*., 2025). Cytogenetic studies also showed that, depending on the concentration and exposure duration, EGL-AgNP induced a significant increase in chromosomal aberrations with a corresponding reduction of mitotic index in human lymphocytes, indicating well as cell cycle delay at high concentrations. These genotoxic stress as the dual functionality of EGL-AgNPs where the anti-microbial results highlight efficacy is to be weighed against possible cell toxicity (Sati *et al*., 2025).

This study emphasizes the necessity of combining optimization synthesis, mechanistic investigation and bioactivity the relevance of green-synthesized nanoparticles. The EGL-AgNPs measurement in assessing possess good controlled physicochemical parameters and potent antimicrobial demonstrate a dose-dependent cytogenotoxic effect activity, although they also that requires strategic dosing for optimization. In creating this fine equilibrium between effectiveness and safety, the current study provides plant-mediated silver salient information in design and development of nanoparticles toward future medical/bacterial applications.

Conclusion

The study developed a novel, for biosynthesis of silver nanoparticles by efficient and green protocol employing *Elaeocarpus ganitrus* leaf extract. Biologically, the bio-processed AgNPs showed significant dose-dependent antibacterial activity in inhibiting bacterial growth to ~ 20% at higher concentrations and were highly effective as antifungal agents against *Aspergillus niger* reducing fungal growth to ~ of control. Cytotoxicity testing 30% indicated concentration dependent, mild decreases in human WBCs viability, whereas cytogenetic analysis demonstrated a decrease in mitotic index from 6.0% nanoparticle levels. These results would control to 1.1% at high exposure address the efficacy of *Elaeocarpus ganitrus* leaf–based AgNPs as promising antimicrobial materials with recognizable biosafety restrictions and for their controlled biomedical and nanobiotechnological opening new dimensions purposes.

References

Acharya, C., Mishra, S., Chaurasia, S. K., Pandey, B. K., Dhar, R., & Pandey, J. K. (2025). Synthesis of metallic nanoparticles using biometabolites: mechanisms and applications. *BioMetals*, **38**(1), 21-54.

Adeyemi, J. O., Oriola, A. O., Onwudiwe, D. C., & Oyedeji, A. O. (2022). Plant extracts mediated metal-based nanoparticles: synthesis and biological applications. *Biomolecules*, **12**(5), 627.

Afhkami, F., Ahmadi, P., & Rostami, G. (2025). Cytotoxicity of Different Concentrations of Silver Nanoparticles and Calcium Hydroxide for MC3T3-E1 Preosteoblast Cell Line. *Clinical and experimental dental research*, **11**(1), e70075. https://doi.org/10.1002/cre2.70075

Alavi, M., & Ashengroph, M. (2023). Mycosynthesis of AgNPs: mechanisms of nanoparticle formation and antimicrobial activities. *Expert Review of Anti-Infective Therapy*, **21**(4), 355-363.

Bamal, D., Singh, A., Chaudhary, G., Kumar, M., Singh, M., Rani, N., ... & Sehrawat, A. R. (2021). Silver nanoparticles biosynthesis, characterization, antimicrobial activities, applications, cytotoxicity and safety issues: An updated review. *Nanomaterials*, **11**(8), 2086.

Breijyeh, Z., & Karaman, R. (2023). Design and synthesis of novel antimicrobial agents. *Antibiotics*, **12**(3), 628.

Chiorcea-Paquim, A. M. (2023). Electrochemistry of flavonoids: a comprehensive review. *International journal of molecular sciences*, **24**(21), 15667.

El-Hussein, A., Mounir, M., El-Sayed, M. A., & Abd El-sadek, M. S. (2024). Green synthesis of nano materials and their applications. In *Comprehensive Analytical Chemistry* (Vol. 105, pp. 461-491). Elsevier.

Godeto, Y. G., Ayele, A., Ahmed, I. N., Husen, A., & Bachheti, R. K. (2023). Medicinal plant-based metabolites in nanoparticles synthesis and their cutting-edge applications: an overview. *Secondary metabolites from medicinal plants*, 1-34.

Hosny, S., Gaber, G. A., Ragab, M. S., Ragheb, M. A., Anter, M., & Mohamed, L. Z. (2025). A Comprehensive Review of Silver Nanoparticles (AgNPs): Synthesis Strategies, Toxicity Concerns, Biomedical Applications, AI-Driven Advancements, Challenges, and Future Perspectives. *Arabian Journal for Science and Engineering*, 1-48.

Jahangirian, H., Shameli, K., Izadiyan, Z., & Kartouzian, A. (2025). Green Synthesis of Nanoparticles Using Dandelion Extract for Biomedical Applications. *Journal of Research in Nanoscience and Nanotechnology*, **16**(1), 9-25.

Khodape, P., Agrawal, A., & Bhurat, M. (2024). Rudraksha (Elaeocarpus ganitrus Roxb) From Divine Miracles to Pharmaceutical Innovations for Medicinal Properties. *Clinical Endocrinology and Metabolism*, **3**(3).

Kirubakaran, D., Wahid, J. B. A., Karmegam, N., Jeevika, R., Sellapillai, L., Rajkumar, M., & SenthilKumar, K. J. (2026). A comprehensive review on the green synthesis of nanoparticles: advancements in biomedical and environmental applications. *Biomedical Materials & Devices*, **4**(1), 388-413.

Lasmi, F., Hamitouche, H., Laribi-Habchi, H., Benguerba, Y., & Chafai, N. (2025). Silver Nanoparticles (AgNPs), Methods of Synthesis, Characterization, and Their Application: A Review. *Plasmonics*, 1-34.

Malik, S., Muhammad, K., & Waheed, Y. (2023). Nanotechnology: a revolution in modern industry. *Molecules*, **28**(2), 661.

Mohan, A., Rajendran, S., & Palani, N. (2025). Sustainable synthesis of iron oxide nanoparticles using phytochemicals: mechanisms, functionalization strategies, applications and future perspectives. *Material Sci & Eng*, **9**(2), 36-54.

Pasieczna-Patkowska, S., Cichy, M., & Flieger, J. (2025). Application of Fourier transform infrared (FTIR) spectroscopy in characterization of green synthesized nanoparticles. *Molecules*, **30**(3), 684.

RaviPadma, K., & Don, K. R. (2025). Pharmacological Insights and Therapeutic Value of Rudraksha: Scientific Review. *Journal of Biochemical Technology*, **16**(2-2025), 93-104.

Sati, A., Ranade, T. N., Mali, S. N., Ahmad Yasin, H. K., & Pratap, A. (2025). Silver nanoparticles (AgNPs): comprehensive insights into bio/synthesis, key influencing factors, multifaceted applications, and toxicity- a 2024 update. *ACS omega*, *10*(8), 7549-7582.

Singh, Y. R., Selvam, A., Lokhande, P. E., & Chakrabarti, S. (2023). Sustainability: an emerging design criterion in nanoparticles synthesis and applications. *Bioinspired and Green Synthesis of Nanostructures: A Sustainable Approach*, 65-113.